Published in final edited form as:
Biotechnol Bioeng. 2010 May 1; 106(1): 149–160. doi:10.1002/bit.22645.

Semi-Permeable Membrane Retention of Synovial Fluid Lubricants Hyaluronan and Proteoglycan 4 for a Biomimetic Bioreactor

Megan E. Blewis[1], **Brian J. Lao**[1], **Kyle D. Jadin**[2], **William J. McCarty**[1], **William D. Bugbee**[3], **Gary S. Firestein**[4], and **Robert L. Sah**[1,5]

Robert L. Sah: rsah@ucsd.edu

[1] Department of Bioengineering, University of California-San Diego, 9500 Gilman Dr., Mail Code 0412, La Jolla, California 92093-0412; telephone: 858-534-0821; fax: 858-822-1614

[2] W.L. Gore & Associates, Inc., Flagstaff, Arizona

[3] Department of Orthopaedic Surgery, University of California-San Diego, School of Medicine, San Diego, California

[4] Division of Rheumatology, Allergy and Immunology, University of California-San Diego, School of Medicine, La Jolla, California

[5] Center for Musculoskeletal Research and Whitaker Center for Biomedical Engineering, Institute of Engineering in Medicine, University of California-San Diego, La Jolla, California

Abstract

Synovial fluid (SF) contains lubricant macromolecules, hyaluronan (HA), and proteoglycan 4 (PRG4). The synovium not only contributes lubricants to SF through secretion by synoviocyte lining cells, but also concentrates lubricants in SF due to its semi-permeable nature. A membrane that recapitulates these synovium functions may be useful in a bioreactor system for generating a bioengineered fluid (BF) similar to native SF. The objectives were to analyze expanded polytetrafluoroethylene membranes with pore sizes of 50 nm, 90 nm, 170 nm, and 3 μm in terms of (1) HA and PRG4 secretion rates by adherent synoviocytes, and (2) the extent of HA and PRG4 retention with or without synoviocytes adherent on the membrane. *Experiment 1*: Synoviocytes were cultured on tissue culture (TC) plastic or membranes ± IL-1β + TGF-β1 + TNF-α, a cytokine combination that stimulates lubricant synthesis. HA and PRG4 secretion rates were assessed by analysis of medium. *Experiment 2*: Bioreactors were fabricated to provide a BF compartment enclosed by membranes ± adherent synoviocytes, and an external compartment of nutrient fluid (NF). A solution with HA (1 mg/mL, MW ranging from 30 to 4,000 kDa) or PRG4 (50 μg/mL) was added to the BF compartment, and HA and PRG4 loss into the NF compartment after 2, 8, and 24 h was determined. Lubricant loss kinetics were analyzed to estimate membrane permeability. *Experiment 1*: Cytokine-regulated HA and PRG4 secretion rates on membranes were comparable to those on TC plastic. *Experiment 2*: Transport of HA and PRG4 across membranes was lowest with 50 nm membranes and highest with 3 μm membranes, and transport of high MW HA was decreased by adherent synoviocytes (for 50 and 90 nm membranes). The permeability to HA mixtures for 50 nm membranes was ~20×10^{-8} cm/s (− cells) and ~5×10^{-8} cm/s (+ cells), for 90 nm membranes was ~35×10^{-8} cm/s (− cells) and ~ 19×10^{-8} cm/s (+ cells), for 170 nm membranes was ~74×10^{-8} cm/s (± cells), and for 3 μm membranes was ~139×10^{-8} cm/s (± cells). The permeability of 450 kDa HA was ~40× lower than that of 30 kDa HA for 50 nm

Correspondence to: Robert L. Sah, rsah@ucsd.edu.

membranes, but only ~2.5× lower for 3 μm membranes. The permeability of 4,000 kDa HA was ~250× lower than that of 30 kDa HA for 50 nm membranes, but only ~4× lower for 3 μm membranes. The permeability for PRG4 was ~4×10^{-8} cm/s for 50 nm membranes, ~48×10^{-8} cm/s for 90 nm membranes, ~144×10^{-8} cm/s for 170 nm membranes, and ~336×10^{-8} cm/s for 3 μm membranes. The associated loss across membranes after 24 h ranged from 3% to 92% for HA, and from 3% to 93% for PRG4. These results suggest that semi-permeable membranes may be used in a bioreactor system to modulate lubricant retention in a bioengineered SF, and that synoviocytes adherent on the membranes may serve as both a lubricant source and a barrier for lubricant transport.

Keywords

synovial fluid; hyaluronan; proteoglycan 4; synoviocytes; semi-permeable membrane; expanded polytetrafluoroethylene (ePTFE)

Introduction

The synovial joint functions as a low-friction, low-wear load-bearing system that includes synovial fluid (SF), contained between articular cartilage and synovium tissue components. Articular cartilage is composed of chondrocytes within a dense extracellular matrix, and bears load and slides relative to an apposing surface. Its low-friction, low-wear properties are due, in part, to lubricant macromolecules in SF, which include hyaluronan (HA) and proteoglycan 4 (PRG4). HA is a glycosaminoglycan comprised of the repeating disaccharide D-glucuronic acid and D-*N*-acetylglucosamine. PRG4 (also called lubricin or SZP) is a mucinous glycoprotein with O-linked β-(1–3)-Gal-GalNAc oligosaccharides (Swann et al., 1981). HA is present in normal SF at a concentration of ~1–4 mg/mL (Balazs, 1974; Dahl et al., 1985), while PRG4 is present at ~0.05–0.5 mg/mL (Schmid et al., 2001). SF HA is present primarily (~70%) at a high (≥4,000 kDa) molecular weight (MW), and ~30% at lower MWs of ~100–4,000 kDa (Lee and Cowman, 1994). PRG4 MW is commonly reported at ~200–400 kDa (Su et al., 2001; Swann et al., 1985). The effective radius, or radius of gyration, for high MW HA is ~100–200 nm (Coleman et al., 2000; Gribbon et al., 1999); that for PRG4 is estimated at ~15–20 nm based on its MW (Flory, 1971).

The synovium not only contributes lubricants to SF through secretion by synoviocyte lining cells, but also concentrates lubricants in SF due its semi-permeable nature (Blewis et al., 2007). HA is secreted by fibroblast-like synoviocytes in synovium (referred to here as “synoviocytes”) (Smith and Ghosh, 1987), while PRG4 is secreted by both chondrocytes in the superficial layer of cartilage as well as synoviocytes. Lubricants are lost from SF, in part due to transport across the synovium. The synovium cellular intima is ~50 μm thick in humans, and the cells form a nearly continuous layer (Knight and Levick, 1984; McDonald and Levick, 1988) attached to an extracellular matrix with an effective pore size of ~20–90 nm (Granger and Taylor, 1975; Sabaratnam et al., 2005). Molecules that transgress the synovium intima enter the underlying subsynovium and are cleared by lymphatics (Jensen et al., 1993; Levick, 1980).

While experimental culture systems have been developed to mimic certain features of the synovial joint to facilitate study of the biology and mechanobiology of synovium and cartilage, a fluid with lubricant function similar to that of native SF has not yet been generated in bioreactor. A 3-D synovium-like tissue has been generated in vitro to study synoviocyte function in organizing the synovium (Kiener et al., 2006). Chondrocytes and synoviocytes have been co-cultured to study cartilage matrix metabolism (Fell and Jubb, 1977; Nixon et al., 2005). Mechanical regulation of joint tissues has been examined at the

scale of osteochondral fragments (Thibault et al., 2002; Visser et al., 1994) and whole joints (Nugent-Derfus et al., 2007). The homeostasis of lubricating fluid may be particularly relevant to mechanobiological bioreactors where cartilaginous surfaces articulate and undergo joint-like motion (Grad et al., 2006; Nugent-Derfus et al., 2007). A semi-permeable membrane with attached synoviocytes could be a useful component of such a bioreactor system.

Membranes with a variety of filtration properties are used for separation of biological molecules (Charcosset, 2006; Saxena et al., 2009) and might be suitable for creating a functional synovium. Expanded polytetrafluoroethylene (ePTFE) is one such candidate material, as it is commonly used in vascular grafts and can be engineered with varying pore size and thus varying solute permeability. It has a controlled structure and is resistant to degradation, properties that may facilitate consistent filtration during extended usage. While solute diffusion across ePTFE membranes has been assessed (Noh et al., 2006), no reports have described PRG4 transport across any type of membrane, and transport of HA has been assessed primarily across native synovium (Coleman et al., 2000; Sabaratnam et al., 2004; Scott et al., 2000b). Additionally, ePTFE has been used as a substrate for cell growth, with surface modification to facilitate cell attachment (Bellon et al., 1993; Walluscheck et al., 1996); however, culture and analysis of lubricant-secreting cell types on ePTFE has not previously been described.

Incorporation of semi-permeable membranes in a bioreactor system may allow retention of lubricants in a pore-size dependent manner, while adherent lubricant-secreting cells may aid in lubricant retention and serve as a lubricant source. Thus, the objectives of this study were to analyze ePTFE membranes of pore sizes 50 nm, 90 nm, 170 nm, and 3 μm in terms of (1) HA and PRG4 secretion rates by adherent synoviocytes, and (2) the extent of HA and PRG4 retention with or without adherent synoviocytes.

Methods

General Methods

Biomimetic Transport Chambers—Transport chambers were biomimetically designed, scaling the native joint as a template. The design consisted of two compartments, denoted as (1) a bioengineered fluid (BF) compartment and (2) a nutrient fluid (NF) compartment, separated by a semi-permeable membrane of surface area 1 cm^2 (Fig. 1). Fluid volumes in BF and NF compartments were 0.1 and 3 mL, respectively (described below). Chambers were made from polysulphone material.

Semi-Permeable Membrane—Poly-L-lysine coated ePTFE membranes (W.L. Gore & Associates, Inc., Flagstaff, AZ) were utilized to separate BF and NF compartments in the bioreactors. As synovium pore size is estimated at ~20–90 nm (Sabaratnam et al., 2004, 2005), membranes of near-equivalent pore size and of larger pore size were used to obtain a range of experimental responses. Membranes had pore sizes averaging ~50 nm, ~90 nm, ~170 nm, and ~3 μm, and thicknesses of ~10–30 μm.

Synoviocyte Isolation—Human synovial tissue was collected with IRB approval and informed donor consent, and studies were approved by the University of California, San Diego Human Subjects Research Protection Program. Tissue was obtained from patients with osteoarthritis (OA) or rheumatoid arthritis (RA) at the time of joint replacement, as described previously (Alvaro-Gracia et al., 1990). RA diagnosis conformed to the 1987 revised American College of Rheumatology criteria (Arnett et al., 1988). Synovial tissues were minced, incubated with 1 mg/mL collagenase in DMEM for 2 h at 37°C, filtered and washed, then incubated in DMEM + 10% FBS. After overnight culture, nonadherent cells

were removed. Adherent cells were later trypsinized, split at a 1:3 ratio, and cultured in DMEM + 10% FBS. Synoviocytes were used from passages 3 to 9 when they are a homogeneous population of fibroblast-like synoviocytes (Alvaro-Gracia et al., 1990).

Experimental Design

Lubricant Secretion by Synoviocytes Attached to Membranes—Synoviocytes were applied to ePTFE membranes of pore size 50 nm, 90 nm, 170 nm, and 3 μm to assess proliferation and lubricant secretion rates, in comparison to those on tissue culture (TC) plastic. Synoviocytes were seeded onto 1 cm^2 membranes at a density of 10,000 cells/cm^2, cultured within the BF compartment of bioreactors in DMEM + 10% FBS for 6 days, and upon reaching confluency (~30,000 cells/cm^2) were then cultured in DMEM + 0.5% FBS for 2 days. This period of serum starvation minimizes proliferation while permitting a robust response to exogenous cytokines (Sundarrajan et al., 2003). Confluent cells were then cultured for an additional 3 days in DMEM + 0.5% FBS (control) ± a cytokine combination, IL-1β (10 ng/mL), TGF-β1 (10 ng/mL), and TNF-α (100 ng/mL) (abbreviated as ITT), that stimulates HA and PRG4 synthesis (Blewis et al., 2009).

Lubricant secretion was assessed after the 3-day ITT cytokine treatment by analyzing medium for HA by an enzyme-linked binding assay using HA binding protein (Afify et al., 2007), and for human PRG4 by ELISA using mAb GW4.23 (a gift from Dr. Klaus Kuettner; Su et al., 2001). Secretion rates were determined by normalizing total mass of secreted lubricant to culture duration and cell number on the final day of culture (i.e., cell number after 3-day treatment with control or ITT media). As minimal proliferation (i.e., ≤20% increase in cellularity) occurred during the 3-day treatment, the cell number obtained at the end of culture was representative of the cell number throughout this period. Cell numbers were determined by solubilizing cell layers with 0.5 mg/mL proteinase K (Roche, Indianapolis, IN), analyzing the solution for DNA using PicoGreen® (McGowan et al., 2002) (Molecular Probes, Eugene, OR), and converting DNA to cell number assuming 7.7 pg DNA/cell (Kim et al., 1988).

Lubricant Flux Across Membranes in Transport Chambers—Lubricant flux across membranes was analyzed using bioreactors with ePTFE membranes alone or with cultured cells. For the latter, synoviocytes were cultured on ePTFE membranes of pore size 50 nm, 90 nm, 170 nm, and 3 μm within the BF compartment of bioreactors in DMEM + 10% FBS for 6 days, and then in DMEM + 0.5% FBS for 2 days. An HA or PRG4 solution was then added to the BF compartment, and DMEM was added in the NF compartment. Bioreactors were incubated at 37°C and 5% CO_2 with gentle mixing for 2, 8, and 24 h. After 2 and 8 h, NF (but not BF) was collected and replenished. After 24 h, both NF and BF were collected for lubricant analysis. Although analysis of BF was not performed at the 2 and 8 h time points, the lubricant present in BF at these time points was determined assuming that the total present in the system was the sum of that in all NF collections and in the BF at the final 24 h time point. The total recovery of HA or PRG4 lubricant from all of the collected solutions averaged 95% of the amount added, indicating this analysis approach was reasonable.

The HA solution was prepared to 1 mg/mL with a MW distribution similar to that of normal SF where ~70% is at high MWs of ~4,000 kDa and ~30% is distributed at lower MWs (Lee and Cowman, 1994). The solution consisted of the following MWs and concentrations, each reconstituted in DMEM: 4,000 kDa (0.7 mg/mL) and 2,400, 1,156, 450, 262, 160, and 30 kDa (each at 0.05 mg/mL) (Associates of Cape Cod, East Falmouth, MA).

The PRG4 solution was prepared to 50 μg/mL using PRG4 purified from bovine cartilage explants. PRG4 was purified from medium conditioned for 12 days by cartilage explants

incubated in DMEM + 0.01% BSA + 10 ng/mL TGF-β1 + 25 μg/mL to stimulate chondrocyte PRG4 secretion (Schmidt et al., 2008). Conditioned media was ultrafiltrated with a 100 kDa MWCO centrifugal filtration device (Millipore, Billerica, MA), treated with *Streptomyces hyaluronidase* (1 U/mL) (Seikagaku Corp., Tokyo, Japan) overnight at 37°C, and then subjected to a second ultrafiltration with a 100 kDa MWCO centrifugal filtration device to remove HA and the *S. hyaluronidase*. PRG4 concentration was then assessed by ELISA (described below), and reconstituted in DMEM to a physiological concentration of 50 μg/mL (Schmid et al., 2001).

To assess overall HA and PRG4 lubricant loss from BF into NF, the collected NF solutions and the residual BF solutions were analyzed for either HA or PRG4 according to which lubricant was being studied (i.e., had been added). Samples were analyzed for HA by an enzyme-linked binding assay using HA binding protein (Afify et al., 2007) and for bovine PRG4 by ELISA using mAb 3-A-4 (gift from Dr. Bruce Caterson; Schumacher et al., 1994). The % of lubricant loss at 2, 8, and 24 h for each condition was calculated by dividing the cumulative lubricant loss at the respective time point by the total lubricant mass collected. Also, the % of lubricant remaining at 2, 8, and 24 h was calculated as 100% minus the cumulative % loss at that time point, where the 100% value at time 0 represented the total lubricant in the system. Overall, the percentage of HA and PRG4 loss across membranes did not appear to be affected by the possible binding of lubricants to the membrane and/or cell layer, as the total recovery of lubricant from all of the collected solutions was ~95% of the amount added.

To further analyze HA transport as a function of MW, the distribution of HA in the 7 MW components in BF and NF samples was determined. Using a gel electrophoresis technique (Lee and Cowman, 1994), 1.5 μg of HA from NF samples collected at 2, 8, and 24 h and from BF collected at 24 h were applied to 1% agarose gels (Lonza, Rockland, ME), separated by horizontal electrophoresis at 100 V for 110 min in TAE buffer (0.4 M Tris–acetate, 0.01 M EDTA, pH 8.3), and visualized after incubation with 0.1% Stainsall (Sigma, St. Louis, MO). Gel images were digitized with a D80 digital camera (Nikon, Melville, NY) and processed to determine the % contribution for each of the 7 MWs. These % contributions were then multiplied by the total loss of HA mass at 2, 8, and 24 h to determine loss of mass for each MW. Finally, the % of total lubricant loss was calculated and presented as described above for the HA mixture.

Engineering Analysis of Membrane

Permeability to Lubricants—The permeability of membranes ± adherent cells to the lubricant *i*, where *i* = HA or PRG4, during lubricant transport studies was estimated by obeying Fick's law, as done in previous studies assessing solute diffusion across a cell-laden membrane (Albelda et al., 1988; Jo et al., 1991; Noh et al., 2006; Sahagun et al., 1990). With sample agitation, the fluid compartments were assumed to be well mixed. The expression for lubricant flux is:

$$\frac{\partial M_i}{\partial t} = AD_i \frac{\partial c_i}{\partial x} \tag{1}$$

where $\partial M_i/\partial t$ is the mass flux of lubricant across the membrane in units of mass per time, A the surface area of membrane in units of length squared, D_i the diffusivity of the lubricant in units of length squared per time, c_i the concentration of lubricant within the membrane, and x the position within the membrane. It should be noted that endogenous lubricant secretion by adherent cells may affect the concentration of lubricant within the membrane, and therefore the mass flux of lubricants; however, as the endogenous secretion in the transport

portion of this study was known a priori to be negligible under the basal media conditions utilized (i.e., <1% of exogenously added lubricant; Blewis et al., 2009), this contribution was assumed to be negligible in the analysis (see Discussion Section).

The permeability P_i is related to membrane and solute properties by:

$$P_i = \frac{D_i}{\Delta x} \tag{2}$$

which can be combined with Equation (1) to yield:

$$\frac{dM_i}{dt} = P_i A \Delta c_i \tag{3}$$

Assuming the concentration of lubricant in the NF compartment (c_i^{NF}) is $\ll$ the concentration in the BF compartment (c_i^{BF}), Equation (3) can be simplified as follows:

$$\Delta c_i = c_i^{BF} - c_i^{NF} \approx c_i^{BF} \tag{4}$$

$$\frac{dM_i}{dt} = P_i A c_i^{BF} \tag{5}$$

The rate of loss in M_i is balanced by the rate of change in $c_{i,BF}$ within the volume (V_{BF}):

$$\frac{dM_i}{dt} = -V^{BF}\left(\frac{dc_i^{BF}}{dt}\right) \tag{6}$$

Combining Equations (5) and (6) results in the following first-order differential equation:

$$-V^{BF}\left(\frac{dc_i^{BF}}{dt}\right) = P_i A c_i^{BF} \tag{7}$$

which can be rearranged to:

$$\frac{dc_i^{BF}}{dt} = -\frac{P_i A}{V^{BF}} c_i^{BF} \tag{8}$$

and the form of the solution to this equation is (where $C_{i,0}^{BF}$ is a constant):

$$c_i^{BF}(t) = C_{i,0}^{BF} e^{-\left(\frac{P_i A}{V^{BF}}\right)t} \tag{9}$$

The above expression was utilized to estimate the membrane permeability to the various lubricants, that is, the mixture of HA MWs, HA of individual MWs, and PRG4. To do so,

the lubricant mass in BF versus time (with time points of 0, 2, 8, 24 h) was first fit with an exponential curve, with R^2 values in the range of ~0.75–0.99. Then, the exponential coefficient (1/τ) from the equation of fit was used with values for A and V_{BF} to calculate permeability as follows:

$$P_i = \frac{V^{BF}}{A\tau} \tag{10}$$

Statistical Analysis

Data are expressed as mean ± SEM. For lubricant secretion studies, data were log transformed to improve normality, and a 1-way ANOVA was used with Tukey post hoc tests to determine the effect of cytokines. For all lubricant transport studies (i.e., those assessing either % of lubricant loss or lubricant permeability), a 1-way ANOVA was used to determine the effect of membrane pore size on % of total loss on total HA (i.e., the mixture of MWs) and PRG4. A *t*-test was also used for each membrane pore size to determine the effect of adherent cells, as such statistical analysis accounts well for the variability of samples being compared. For analysis of specific HA MWs, a 3-way ANOVA was used to determine individual and interactive effects of membrane pore size, HA MW, and adherent cells, since effects of multiple HA MWs were being assessed. For the % of loss analysis, data from 24 h were used and arcsine transformed to normalize data since %'s form binomial rather than normal distributions (Sokal and Rohlf, 1995). For permeability analysis, data were log transformed.

Results

Synoviocyte Lubricant Secretion on Membranes

Synoviocytes remained viable on ePTFE and proliferated over 6 days to a greater extent on 50 and 90 nm membranes than on TC plastic (~3× vs. ~2×; $P < 0.05$, Fig. 2A). Synoviocyte secretion of HA was stimulated by the ITT cytokine combination for all substrates ($P < 0.05$, Fig. 2B). The average HA secretion rate induced by ITT was ~150 μg/(10^6 cell day), a marked ~60× increase over basal controls. Secretion of PRG4 by synoviocytes on TC plastic and 50, 90, and 170 nm membranes exhibited a similar trend of ITT responsiveness (Fig. 2C). The secretion of PRG4 and that of HA were correlated positively (Fig. 2D).

Lubricant Flux Across Membranes in Transport Chambers

The loss of HA across membranes was dependent upon pore size as well as the presence of adherent cells for certain pore size membranes. The average % of total HA loss (with the mixture of MWs) from BF to NF after 24 h was ~10% for 50 nm membranes, ~21% for 90 nm membranes, 36% for 170 nm membranes, and ~66% for 3 μm membranes (Fig. 3A). The % loss from 3 μm membranes was greater than that of all other membranes ($P < 0.05$), and the % loss from 170 nm membranes was greater than that of 50 nm membranes. The presence of adherent cells led to decreased HA loss for the small pore size membranes (16% vs. 4% for 50 nm and 26% vs. 15% for 90 nm, $P < 0.05$).

HA loss was further dependent upon MW, and there was a significant interaction with membrane pore size ($P < 0.05$) (Fig. 4). 30 kDa HA had a high % loss after 24 h (~92%) that was similar for all pore size membranes (Fig. 4G). 160 kDa HA was lost to a greater extent from 90 (60%), 170 (70%), and 3 μm (83%) membranes than from 50 nm membranes (29%) ($P < 0.05$) (Fig. 4F). 262 and 450 kDa HA similarly had the least % loss from 50 nm membranes compared to all others ($P < 0.05$), but there was also a greater loss of each from 3 μm (37%, 54%) than from 90 nm membranes (13%, 16%) ($P < 0.05$) (Fig. 4D and E).

1,156, 2,400, and 4,000 kDa HA were all lost from BF to a similar extent by the membranes, with a significantly greater % loss from 3 μm membranes (~61%) than 50 (~5%), 90 (~12%), and 170 nm membranes (~29%) ($P < 0.05$) (Fig. 4A–C). 1,156 and 2,400 kDa HA were also lost to a greater extent from 170 nm membranes than from 50 nm membranes ($P < 0.05$). The presence of adherent cells decreased the % of HA loss from BF for 50 and 90 nm pore size membranes ($P < 0.05$).

PRG4 loss across membranes was dependent upon pore size, but unaffected by adherent cells. The % loss from BF to NF after 24 h was ~3% for 50 nm membranes, ~28% for 90 nm membranes, 67% for 170 nm membranes, and ~93% for 3 μm membranes (Fig. 3B). The % loss from each membrane was significantly different than that of all other membranes ($P < 0.05$).

Permeability of Membranes to Lubricants

Reduction of experimental data according to the engineering analysis yielded values for lubricant permeability through membranes ± adherent cells (Figs. 5 and 6, Table I). Figure 7 shows representative curves of the lubricant mass in BF vs. time that were fit with an exponential curve predicted by the engineering analysis to estimate permeability (R^2 values were in the range of ~0.75–0.99).

The permeability of membranes to HA was dependent upon pore size, as well as the presence of adherent cells for certain pore size membranes. The average permeability for HA (with the mixture of MWs) was ~12×10^{-8} cm/s for 50 nm membranes, ~27×10^{-8} cm/s for 90 nm membranes, ~74×10^{-8} cm/s for 170 nm membranes, and ~139×10^{-8} cm/s for 3 μm membranes (Fig. 5A, Table I). The permeability of 3 μm membranes was greater than that of all other membranes ($P < 0.05$), and the permeability of 170 nm membranes was greater than that of 50 and 90 nm membranes ($P < 0.05$). The presence of an adherent cell layer led to decreased permeability for small pore size membranes (~20×10^{-8} vs. ~5×10^{-8} cm/s for 50 nm, and ~35×10^{-8} vs. ~19×10^{-8} cm/s for 90 nm, $P < 0.05$).

HA permeability was further dependent upon MW, and there was a significant interaction with membrane pore size ($P < 0.05$) (Fig. 6, Table I). 30 kDa HA had a high permeability (~373×10^{-8} cm/s) and was similar for all pore size membranes, in contrast to the permeability for all other MWs (Fig. 6G). For example, permeability for 160 kDa HA was ~4–5× lower for 50 nm membranes than for 170 nm and 3 μm membranes (45×10^{-8} vs. 158×10^{-8} and 231×10^{-8} cm/s, respectively) ($P < 0.05$) (Fig. 6F). Additionally, the permeability for 262, 450, and 1,156 kDa HA was ~3–15× lower for 50 nm membranes compared to all other membranes ($P < 0.05$) (Fig. 6C–E). In a similar manner, for 2,400 and 4,000 kDa HA, the permeability of 50 nm membranes (~5×10^{-8} cm/s) was ~2–30× lower than that of all other membranes, and the permeability of 3 μm membranes (~113×10^{-8} cm/s) was ~3–30× higher than that of all other membranes ($P < 0.05$) (Fig. 6A,B). In comparing HA of different MWs across the same pore size membrane, the permeability of 450 kDa HA was ~40× lower than that of 30 kDa HA for 50 nm membranes, but only ~2.5× lower for 3 μm membranes. The permeability of 4,000 kDa HA was ~250× lower than that of 30 kDa HA for 50 nm membranes, but only ~4× lower for 3 μm membranes. The presence of an adherent cell layer significantly affected the permeability of both 50 and 90 nm pore size membranes (~12× and ~2× lower permeability, respectively, $P < 0.05$).

PRG4 permeability was dependent upon pore size, but unaffected by adherent cells. Permeability was ~4×10^{-8} cm/s for 50 nm membranes, ~48×10^{-8} cm/s for 90 nm membranes, ~144×10^{-8} cm/s for 170 nm membranes, and ~336×10^{-8} cm/s for 3 μm membranes (Fig. 5B, Table I). The permeability of 3 μm membranes was greatest, and the

permeability of 170 nm membranes was greater than that of 50 and 90 nm membranes ($P < 0.05$).

Discussion

This study examined HA and PRG4 secretion rates by synoviocytes on ePTFE membranes of pore sizes ~50 nm to ~3 μm, and the extent of HA and PRG4 retention by these membranes. Synoviocyte HA and PRG4 secretion rates on membranes were comparable to those on TC plastic and tended to be stimulated by application of cytokines. Transport of HA and PRG4 across membranes was dependent upon pore size, with % of total lubricant loss and membrane permeability to lubricant being lowest with 50 nm membranes and highest with 3 μm membranes. HA transport was further dependent upon the presence of adherent cells and HA MW, with cells (for 50 and 90 nm membranes) and higher MWs resulting in decreased loss and permeability. These results suggest that membranes of various pore sizes may be applied to a bioreactor system to modulate lubricant composition in a bioengineered SF. Synoviocytes present on membranes may serve as both a lubricant source and a barrier to lubricant transport.

The interpretation of data from the present study applies to synoviocytes isolated from arthritic joints. However, these cells behave similarly to normal synoviocytes in most respects when stimulated by cytokines, including proliferation, metalloproteinase production, adhesion molecule expression, and activation of the mitogen-activated kinase pathways (Bartok and Firestein, 2009; Firestein, 1996). While some differences have been observed in a SCID mouse model containing cartilage explants (Geiler et al., 1994), these properties were not examined in the present studies. However, those observations probably have less relevance considering that the mechanisms of adhesion to cartilage in the murine model are not necessarily relevant to the normal synovial matrix. These considerations, along with difficulty obtaining well-characterized fibroblast-like synoviocytes from normal individuals, have led most groups studying type B synoviocytes to focus on cells derived from total joint replacement samples.

The assessment of lubricant transport properties was dependent on a number of assumptions. Although a large % of total lubricants diffused across membranes in certain conditions in this study, the assumption that lubricant concentration in NF was negligible compared to BF remained valid due to the relatively large volume of NF (3 mL) compared to BF (0.1 mL) and the replenishment of the NF compartment. For example, even if 70% of a 1 mg/mL HA solution from BF diffused into NF, the concentration in BF would be 0.3 mg/mL and the concentration in NF would be more than 10× lower at 0.023 mg/mL. Also, the endogenous lubricant secretion by synoviocytes during transport studies likely had negligible contribution to the BF lubricant concentration, as basal media conditions were used where lubricant secretion is very low as described in previous studies (Blewis et al., 2009) and as confirmed here. Thus, it is predicted to contribute in a 24 h period a mass that is <1% of that applied exogenously (i.e., synoviocytes are estimated to secrete ~0.3 μg HA vs. 100 μg exogenously applied HA, or ~0.03 μg PRG4 vs. 5 μg exogenously applied PRG4, as calculated using a basal HA secretion rate of ~10 μg/(10^6 cell day), a basal PRG4 secretion rate of ~1 μg/(10^6 cell day), a time period of 1 day, and a total cell number of ~30,000 which represents the confluent cell layer and negligible proliferation in basal media conditions). Furthermore, the synoviocytes utilized in this study were of human origin while the exogenous PRG4 applied to bioreactors was of bovine origin; the use of a bovine-specific PRG4 antibody in the analyses thus eliminated confounding detection of endogenously secreted PRG4. Finally, the recovery of lubricant that was ~95% of that added to the system is consistent with the above, and also suggests that there was negligible binding of lubricants to the membrane.

The ability to culture synoviocytes on material substrates, rather than on standard TC plastic, with maintenance of a desired phenotype is consistent with and extends previous studies (Kiener et al., 2006; Ozturk et al., 2008; Vickers et al., 2004). Synoviocytes attached to ePTFE membranes, proliferated, and maintained secretion of both HA and PRG4 in a manner that appeared to be coordinately regulated by cytokines, with correlated rates of secretion. A thin, flexible lubricant-secreting sheet could be incorporated into various types of joint bioreactors to enclose cartilage surfaces and form a SF compartment, including systems of simple geometry and also complex joint-scale systems with large, contoured cartilage surfaces.

The findings in this study illustrate the importance of MW in HA transport across membranes, and provide an in vitro analog to previous work examining in vivo transport of HA across synovium. Studies that infused HA of varying MW into rabbit knee joints demonstrated that with lower MW HA (~140, ~500 kDa) there was less retention by the synovium and accumulation in SF than with higher MW HA (~2,200 kDa) (Coleman et al., 2000; Sabaratnam et al., 2005). Similar observations were made with infusion of HA into dog knee joints, where 2,300 kDa HA scarcely penetrated synovium, but 840 kDa HA penetrated readily (Asari et al., 1998).

As PRG4 loss across membranes in this study was affected by pore size in a relatively similar manner to that of HA, PRG4 forms of varying MW may also be differentially transported. PRG4 MW in SF is commonly reported at ~345 kDa, although larger multimeric forms (Schmidt et al., 2009) and smaller MW forms may also exist (Swann et al., 1985). The relative abundance of these different MWs in SF and their contribution to PRG4 transport remains to be established, but increases in PRG4 MW would likely decrease the rate of PRG4 loss from SF.

The different molecular structures of HA and PRG4 may account for some differences in transport patterns observed in this study between PRG4 and HA of a similar MW (450 kDa). The % of total PRG4 loss with 50 nm membranes was limited compared to that of 450 kDa HA (3% vs. 12%), while the % loss with 170 nm and 3 μm pore sizes was greater for PRG4 (67% vs. 50% and 93% vs. 74%). Comparison of the permeability values between PRG4 and 450 kDa HA revealed similar distinctions. The large mucin-like domain in the PRG4 structure and potential differences in secondary lubricant structures could contribute to distinct transport properties.

Solute efflux from SF in vivo is a function of both diffusion-driven and convection-driven flux across the synovium, and although many studies have assessed the latter (Coleman et al., 2000; Sabaratnam et al., 2004; Scott et al., 2000a,b), some comparisons may be drawn between permeability values obtained in this in vitro study and the literature. Synovium permeability to HA or PRG4 remains to be measured, but free diffusion coefficients of the lubricants are 0.98×10^{-7} cm^2/s and 1.11×10^{-7} cm^2/s, respectively (Swann et al., 1981; Sabaratnam et al., 2005). The permeability values obtained here for 50 nm membranes, a pore size within synovium range, were ~$1–5 \times 10^{-8}$ cm/s for PRG4 and HA of physiological MW. An estimated restricted diffusion coefficient through the membrane, calculated using these permeability values and a membrane thickness of ~0.02 cm, is ~1×10^{-9} cm^2/s to 2×10^{-10} cm^2/s, expectedly lower than the free diffusion coefficients. Additionally, synovium permeability to albumin, a low MW solute that readily permeates, is expectedly greater than that of HA and PRG4 found here (~6×10^{-5} cm/s vs. ~$1–5 \times 10^{-8}$ cm/s) (Granger and Taylor, 1975). Taken together, some permeability values reported in this study for lubricants with ePTFE membranes, particularly the 50 nm pore size, appear within range of synovium lubricant permeability.

As in vivo alterations in synovium structure may occur in disease or injury to affect lubricant loss from SF, the range of membrane pore sizes utilized in this study provide an analog to various in vivo conditions. For example, a decrease in the half-life of HA in SF is often observed in arthritic joints compared to normal joints (~12 h vs. ~24 h) (Coleman et al., 1997; Fraser et al., 1993; Laurent et al., 1992; Sakamoto et al., 1984), as are increases in the concentration of certain SF cytokines that may contribute to degradation of the synovium matrix and an increase in synovium permeability (Bertone et al., 2001; Coleman et al., 1998; Joosten et al., 2006; Kotake et al., 1999; Marks and Donaldson, 2005; Scott et al., 1998). If 50 nm pore size membranes mimic certain transport properties of normal synovium, then membranes of pore sizes 90 nm to 3 μm may mimic the altered transport properties of pathological synovium, with varying degrees of increased permeability. Native synovium tissue from either normal or pathological joints might be performed as a comparison in the current experimental system, although the isolation of tissue suitable for such analysis may be difficult. The altered transport properties in vivo may also be due to altered MW forms of HA in SF.

The bioreactor system developed here could be utilized to better understand whether lubricant interactions affect their transport properties. HA and PRG4 synergistically interact to lower friction at cartilage–cartilage and latex–glass interfaces, by postulated mechanisms involving molecular interactions (Jay et al., 1992; Schmidt et al., 2007). Such interactions in SF could increase the effective MW of HA and PRG4 and limit lubricant transport across synovium. Physical interactions of lubricants with surrounding joint tissues, such as synovium, may also occur and slow transport. Various biological solutions may be applied to the bioreactor system developed here to study the effects of these different types of interactions on lubricant transport.

The results of this study demonstrate (1) the ability of human synoviocytes to adhere and proliferate on semi-permeable membranes and to be regulated in their lubricant secretion rates by cytokines, and (2) the ability of these membranes, with or without adherent cells, to retain lubricants in a manner dependent upon membrane pore size and lubricant MW. Such membranes may be applied to a joint bioreactor system as a method to modulate lubricant composition in a bioengineered SF. The ability to bioengineer SF may have application in tissue engineering whole joints for biological joint replacement, by providing an appropriate lubricating environment to articulating cartilage surfaces during applied mechanical stimulation in bioreactors. Bioengineering SF in bioreactors may also have applications in developing lubricant supplements for deficient SF, and in identifying molecules involved in lubricant regulation.

Acknowledgments

Contract grant sponsors: AO Foundation, NIH

Contract grant numbers: R01 AR051565; R01 AR055637; P01 AG007996; R01 AI070555; R01 AR047825

The authors thank Josh Hillman for maintaining the human synoviocyte lines and David Boyle for lab management (GSF). This work was supported by the Howard Hughes Medical Institute through an award to UCSD under the HHMI Professor Program (RLS), and by UC Systemwide Biotechnology Research & Education Program GREAT Training Grant 2006-17 (MEB).

References

Afify A, Lynne LC, Howell L. Correlation of cytologic examination with ELISA assays for hyaluronan and soluble CD44v6 levels in evaluation of effusions. Diagn Cytopathol 2007;35(2): 105–110. [PubMed: 17230576]

Albelda SM, Sampson PM, Haselton FR, McNiff JM, Mueller SN, Williams SK, Fishman AP, Levine EM. Permeability characteristics of cultured endothelial cell monolayers. J Appl Physiol 1988;64(1):308–322. [PubMed: 2451657]

Alvaro-Gracia JM, Zvaifler NJ, Firestein GS. Cytokines in chronic inflammatory arthritis. V. Mutual antagonism between interferon-gamma and tumor necrosis factor-alpha on HLA-DR expression, proliferation, collagenase production, and granulocyte macrophage colony-stimulating factor production by rheumatoid arthritis synoviocytes. J Clin Invest 1990;86(6):1790–1798. [PubMed: 2174906]

Arnett FC, Edworthy SM, Bloch DA, McShane DJ, Fries JF, Cooper NS, Healey LA, Kaplan SR, Liang MH, Luthra HS. The American Rheumatism Association 1987 revised criteria for the classification of rheumatoid arthritis. Arthritis Rheum 1988;31(3):315–324. [PubMed: 3358796]

Asari A, Miyauchi S, Matsuzaka S, Ito T, Kominami E, Uchiyama Y. Molecular weight-dependent effects of hyaluronate on the arthritic synovium. Arch Histol Cytol 1998;61(2):125–135. [PubMed: 9650887]

Balazs, EA. The physical properties of synovial fluid and the special role of hyaluronic acid. In: Helfet, AJ., editor. Disorders of the knee. Philadelphia: Lippincott Co; 1974. p. 63-75.

Bartok B, Firestein GS. Fibroblast-like synoviocytes: Key effector cells in rheumatoid arthritis. Immunol Rev. 2009 (in press).

Bellon JM, Bujan J, Honduvilla NG, Hernando A, Navlet J. Endothelial cell seeding of polytetrafluoroethylene vascular prostheses coated with a fibroblastic matrix. Ann Vasc Surg 1993;7(6):549–555. [PubMed: 8123457]

Bertone AL, Palmer JL, Jones J. Synovial fluid cytokines and eicosanoids as markers of joint disease in horses. Vet Surg 2001;30(6):528–538. [PubMed: 11704948]

Blewis ME, Nugent-Derfus GE, Schmidt TA, Schumacher BL, Sah RL. A model of synovial fluid lubricant composition in normal and injured joints. Eur Cell Mater 2007;13:26–39. [PubMed: 17340555]

Blewis ME, Lao BJ, Schumacher BL, Bugbee WD, Firestein GS, Sah RL. Interactive cytokine regulation of synoviocyte lubricant secretion. Tissue Eng. 2009 (Epub ahead of print).

Charcosset C. Membrane processes in biotechnology: An overview. Biotechnol Adv 2006;24(5):482–492. [PubMed: 16687233]

Coleman PJ, Scott D, Ray J, Mason RM, Levick JR. Hyaluronan secretion into the synovial cavity of rabbit knees and comparison with albumin turnover. J Physiol 1997;503(Pt 3):645–656. [PubMed: 9379418]

Coleman PJ, Scott D, Abiona A, Ashhurst DE, Mason RM, Levick JR. Effect of depletion of interstitial hyaluronan on hydraulic conductance in rabbit knee synovium. J Physiol 1998;509(Pt 3):695–710. [PubMed: 9596792]

Coleman PJ, Scott D, Mason RM, Levick JR. Role of hyaluronan chain length in buffering interstitial flow across synovium in rabbits. J Physiol 2000;526(Pt 2):425–434. [PubMed: 10896731]

Dahl LB, Dahl IM, Engstrom-Laurent A, Granath K. Concentration and molecular weight of sodium hyaluronate in synovial fluid from patients with rheumatoid arthritis and other arthropathies. Ann Rheum Dis 1985;44(12):817–822. [PubMed: 4083937]

Fell HB, Jubb RW. The effect of synovial tissue on the breakdown of articular cartilage in organ culture. Arthritis Rheum 1977;20(7):1359–1371. [PubMed: 911354]

Firestein GS. Invasive fibroblast-like synoviocytes in rheumatoid arthritis. Passive responders or transformed aggressors? Arthritis Rheum 1996;39(11):1781–1790. [PubMed: 8912499]

Flory, PJ. Principles of polymer chemistry. Ithaca, NY, USA: Cornell University Press; 1971.

Fraser JR, Kimpton WG, Pierscionek BK, Cahill RN. The kinetics of hyaluronan in normal and acutely inflamed synovial joints: Observations with experimental arthritis in sheep. Semin Arthritis Rheum 1993;22(6 Suppl 1):9–17. [PubMed: 8342053]

Geiler T, Kriegsmann J, Keyszer GM, Gay RE, Gay S. A new model for rheumatoid arthritis generated by engraftment of rheumatoid synovial tissue and normal human cartilage into SCID mice. Arthritis Rheum 1994;37(11):1664–1671. [PubMed: 7526870]

Grad S, Gogolewski S, Alini M, Wimmer MA. Effects of simple and complex motion patterns on gene expression of chondrocytes seeded in 3D scaffolds. Tissue Eng 2006;12(11):3171–3179. [PubMed: 17518631]

Granger HJ, Taylor AE. Permeability of connective tissue linings isolated from implanted capsules; implications for interstitial pressure measurements. Circ Res 1975;36(1):222–228. [PubMed: 1116223]

Gribbon P, Heng BC, Hardingham TE. The molecular basis of the solution properties of hyaluronan investigated by confocal fluorescence recovery after photobleaching. Biophys J 1999;77(4):2210–2216. [PubMed: 10512840]

Jay GD, Lane BP, Sokoloff L. Characterization of a bovine synovial fluid lubricating factor III. The interaction with hyaluronic acid. Connect Tissue Res 1992;28(4):245–255. [PubMed: 1304440]

Jensen LT, Henriksen JH, Olesen HP, Risteli J, Lorenzen I. Lymphatic clearance of synovial fluid in conscious pigs: The aminoterminal propeptide of type III procollagen. Eur J Clin Invest 1993;23(12):778–784. [PubMed: 8143755]

Jo H, Dull RO, Hollis TM, Tarbell JM. Endothelial albumin permeability is shear dependent, time dependent, and reversible. Am J Physiol 1991;260(6 Pt 2):H1992–H1996. [PubMed: 1905493]

Joosten LA, Netea MG, Kim SH, Yoon DY, Oppers-Walgreen B, Radstake TR, Barrera P, van de Loo FA, Dinarello CA, van den Berg WB. IL-32, a proinflammatory cytokine in rheumatoid arthritis. Proc Natl Acad Sci USA 2006;103(9):3298–3303. [PubMed: 16492735]

Kiener HP, Lee DM, Agarwal SK, Brenner MB. Cadherin-11 induces rheumatoid arthritis fibroblast-like synoviocytes to form lining layers in vitro. Am J Pathol 2006;168(5):1486–1499. [PubMed: 16651616]

Kim YJ, Sah RLY, Doong JYH, Grodzinsky AJ. Fluorometric assay of DNA in cartilage explants using Hoechst 33258. Anal Biochem 1988;174(1):168–176. [PubMed: 2464289]

Knight AD, Levick JR. Morphometry of the ultrastructure of the blood-joint barrier in the rabbit knee. Q J Exp Physiol 1984;69(2):271–288. [PubMed: 6729017]

Kotake S, Udagawa N, Takahashi N, Matsuzaki K, Itoh K, Ishiyama S, Saito S, Inoue K, Kamatani N, Gillespie MT, Martin TJ, Suda T. IL-17 in synovial fluids from patients with rheumatoid arthritis is a potent stimulator of osteoclastogenesis. J Clin Invest 1999;103(9):1345–1352. [PubMed: 10225978]

Laurent UB, Fraser JR, Engstrom-Laurent A, Reed RK, Dahl LB, Laurent TC. Catabolism of hyaluronan in the knee joint of the rabbit. Matrix 1992;12(2):130–136. [PubMed: 1603035]

Lee HG, Cowman MK. An agarose gel electrophoretic method for analysis of hyaluronan molecular weight distribution. Anal Biochem 1994;219(2):278–287. [PubMed: 8080084]

Levick JR. Contributions of the lymphatic and microvascular systems to fluid absorption from the synovial cavity of the rabbit knee. J Physiol 1980;306:445–461. [PubMed: 7463369]

Marks PH, Donaldson ML. Inflammatory cytokine profiles associated with chondral damage in the anterior cruciate ligament-deficient knee. Arthroscopy 2005;21(11):1342–1347. [PubMed: 16325085]

McDonald JN, Levick JR. Morphology of surface synoviocytes in situ at normal and raised joint pressure, studied by scanning electron microscopy. Ann Rheum Dis 1988;47(3):232–240. [PubMed: 3355260]

McGowan KB, Kurtis MS, Lottman LM, Watson D, Sah RL. Biochemical quantification of DNA in human articular and septal cartilage using PicoGreen and Hoechst 33258. Osteoarthritis Cartilage 2002;10(7):580–587. [PubMed: 12127839]

Nixon AJ, Haupt JL, Frisbie DD, Morisset SS, McIlwraith CW, Robbins PD, Evans CH, Ghivizzani S. Gene-mediated restoration of cartilage matrix by combination insulin-like growth factor-I/interleukin-1 receptor antagonist therapy. Gene Ther 2005;12(2):177–186. [PubMed: 15578043]

Noh I, Choi YJ, Son Y, Kim CH, Hong SH, Hong CM, Shin IS, Park SN, Park BY. Diffusion of bioactive molecules through the walls of the medial tissue-engineered hybrid ePTFE grafts for applications in designs of vascular tissue regeneration. J Biomed Mater Res A 2006;79(4):943–953. [PubMed: 16941597]

Nugent-Derfus GE, Takara T, O'Neill JK, Cahill SB, Gortz S, Pong T, Inoue H, Aneloski NM, Wang WW, Vega KI, Klein TJ, Hsieh-Bonassera ND, Bae WC, Burke JD, Bugbee WD, Sah RL.

Continuous passive motion applied to whole joints stimulates chondrocyte biosynthesis of PRG4. Osteoarthritis Cartilage 2007;15(5):566–574. [PubMed: 17157538]

Ozturk AM, Yam A, Chin SI, Heong TS, Helvacioglu F, Tan A. Synovial cell culture and tissue engineering of a tendon synovial cell biomembrane. J Biomed Mater Res A 2008;84(4):1120–1126. [PubMed: 18181108]

Sabaratnam S, Mason RM, Levick JR. Filtration rate dependence of hyaluronan reflection by joint-to-lymph barrier: Evidence for concentration polarisation. J Physiol 2004;557(Pt 3):909–922. [PubMed: 15073278]

Sabaratnam S, Arunan V, Coleman PJ, Mason RM, Levick JR. Size selectivity of hyaluronan molecular sieving by extracellular matrix in rabbit synovial joints. J Physiol 2005;567(Pt 2):569–581. [PubMed: 15961430]

Sahagun G, Moore SA, Hart MN. Permeability of neutral vs. anionic dextrans in cultured brain microvascular endothelium. Am J Physiol 1990;259(1 Pt 2):H162–H166. [PubMed: 1695819]

Sakamoto T, Mizono S, Miyazaki K, Yamaguchi T, Toyoshima H, Namiki O. Biological fate of sodium hyaluronate (SPH): Studies on the distribution, metabolism, and excretion of ^{14}C-SPH in rabbits after intra-articular administration. Pharmacometrics 1984;28:375–387.

Saxena A, Tripathi BP, Kumar M, Shahi VK. Membrane-based techniques for the separation and purification of proteins: An overview. Adv Colloid Interface Sci 2009;145(1–2):1–22. [PubMed: 18774120]

Schmid T, Lindley K, Su J, Soloveychik V, Block J, Kuettner K, Schumacher B. Superficial zone protein (SZP) is an abundant glycoprotein in human synovial fluid and serum. Trans Orthop Res Soc 2001;26:82.

Schmidt TA, Gastelum NS, Nguyen QT, Schumacher BL, Sah RL. Boundary lubrication of articular cartilage: Role of synovial fluid constituents. Arthritis Rheum 2007;56(3):882–891. [PubMed: 17328061]

Schmidt TA, Gastelum NS, Han EH, Nugent-Derfus GE, Schumacher BL, Sah RL. Differential regulation of proteoglycan 4 metabolism in cartilage by IL-1a, IGF-I, and TGF-b1. Osteoarthritis Cartilage 2008;16(1):90–97. [PubMed: 17596975]

Schmidt TA, Plaas AH, Sandy JD. Disulfide-bonded multimers of proteoglycan 4 (PRG4) are present in normal synovial fluids. Biochim Biophys Acta 2009;1790:375–384. [PubMed: 19332105]

Schumacher BL, Block JA, Schmid TM, Aydelotte MB, Kuettner KE. A novel proteoglycan synthesized and secreted by chondrocytes of the superficial zone of articular cartilage. Arch Biochem Biophys 1994;311:144–152. [PubMed: 8185311]

Scott D, Coleman PJ, Abiona A, Ashhurst DE, Mason RM, Levick JR. Effect of depletion of glycosaminoglycans and non-collagenous proteins on interstitial hydraulic permeability in rabbit synovium. J Physiol 1998;511(Pt 2):629–643. [PubMed: 9706037]

Scott D, Coleman PJ, Mason RM, Levick JR. Concentration dependence of interstitial flow buffering by hyaluronan in synovial joints. Microvasc Res 2000a;59(3):345–353. [PubMed: 10792965]

Scott D, Coleman PJ, Mason RM, Levick JR. Interaction of intraarticular hyaluronan and albumin in the attenuation of fluid drainage from joints. Arthritis Rheum 2000b;43(5):1175–1182. [PubMed: 10817572]

Smith MM, Ghosh P. The synthesis of hyaluronic acid by human synovial fibroblasts is influenced by the nature of the hyaluronate in the extracellular environment. Rheumatol Int 1987;7(3):113–122. [PubMed: 3671989]

Sokal, RR.; Rohlf, FJ. Biometry. New York: WH Freeman and Co; 1995. p. 887

Su J-L, Schumacher BL, Lindley KM, Soloveychik V, Burkhart W, Triantafillou JA, Kuettner KE, Schmid TM. Detection of superficial zone protein in human and animal body fluids by cross-species monoclonal antibodies specific to superficial zone protein. Hybridoma 2001;20(3):149–157. [PubMed: 11461663]

Sundarrajan M, Boyle DL, Chabaud-Riou M, Hammaker D, Firestein GS. Expression of the MAPK kinases MKK-4 and MKK-7 in rheumatoid arthritis and their role as key regulators of JNK. Arthritis Rheum 2003;48(9):2450–2460. [PubMed: 13130464]

Swann DA, Slayter HS, Silver FH. The molecular structure of lubricating glycoprotein-I, the boundary lubricant for articular cartilage. J Biol Chem 1981;256(11):5921–5925. [PubMed: 7240180]

Swann DA, Silver FH, Slayter HS, Stafford W, Shore E. The molecular structure and lubricating activity of lubricin isolated from bovine and human synovial fluids. Biochem J 1985;225(1):195–201. [PubMed: 3977823]

Thibault M, Poole AR, Buschmann MD. Cyclic compression of cartilage/bone explants in vitro leads to physical weakening, mechanical breakdown of collagen and release of matrix fragments. J Orthop Res 2002;20(6):1265–1273. [PubMed: 12472239]

Vickers SM, Johnson LL, Zou LQ, Yannas IV, Gibson LJ, Spector M. Expression of alpha-smooth muscle actin by and contraction of cells derived from synovium. Tissue Eng 2004;10(7):1214–1223. [PubMed: 15363177]

Visser NA, van Kampen GPJ, Dekoning MHMT, van der Korst JK. The effects of loading on the synthesis of biglycan and decorin in intact mature articular cartilage in vitro. Connect Tissue Res 1994;30(4):241–250. [PubMed: 7956203]

Walluscheck KP, Steinhoff G, Kelm S, Haverich A. Improved endothelial cell attachment on ePTFE vascular grafts pretreated with synthetic RGD-containing peptides. Eur J Vasc Endovasc Surg 1996;12(3):321–330. [PubMed: 8896475]

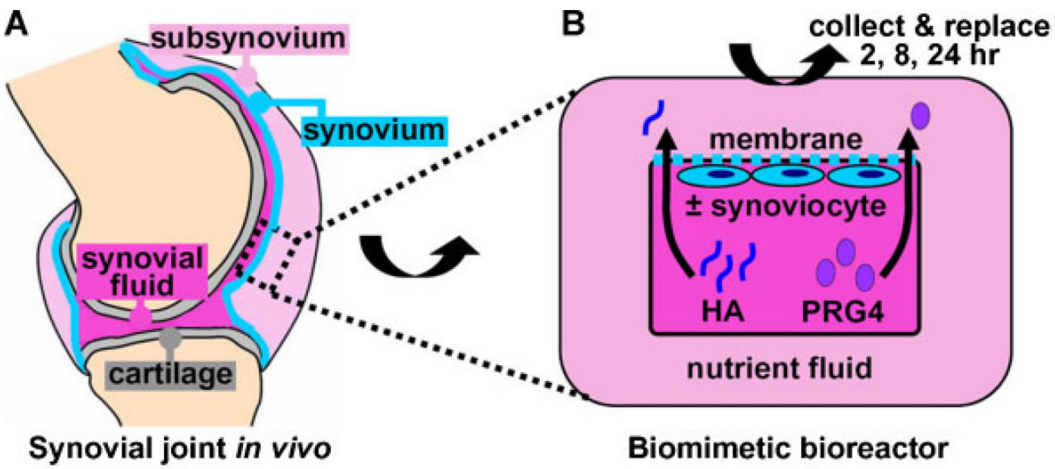

Figure 1.

(**A**) SF lubricant retention by the synovium in the in vivo synovial joint can be (**B**) biomimetically modeled in a bioreactor where a bioengineered (synovial) fluid compartment containing lubricants (HA and PRG4) is separated from a nutrient fluid compartment by a semi-permeable membrane ± adhered synoviocytes. [Color figure can be seen in the online version of this article, available at www.interscience.wiley.com.]

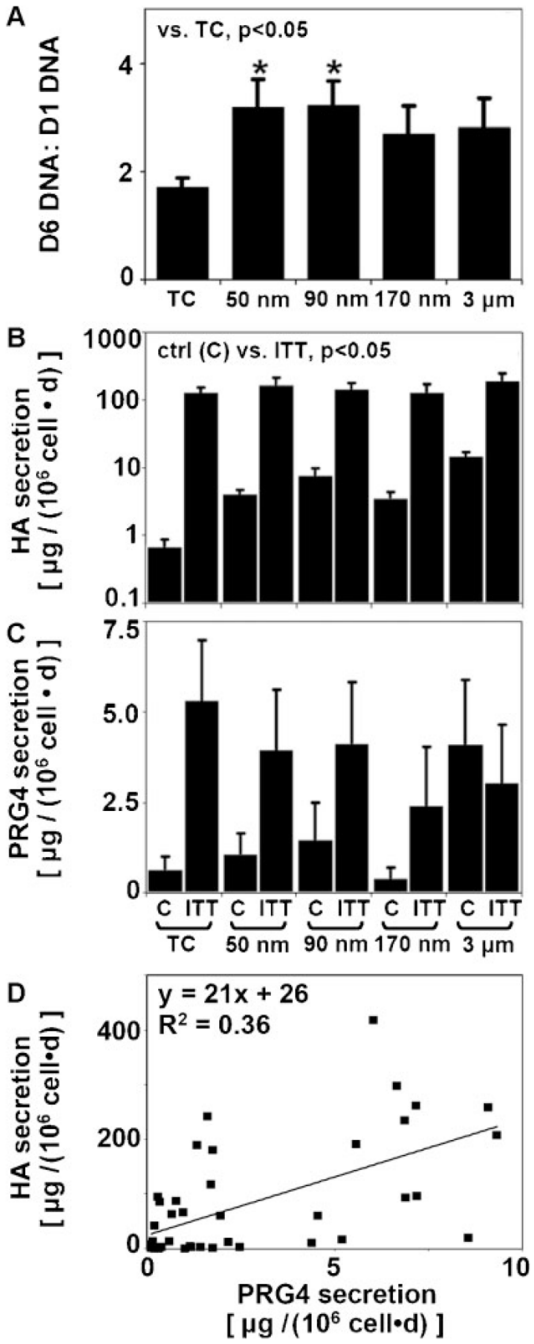

Figure 2.

(**A**) Effects of substrate on synoviocyte proliferation over a 6-day culture period. Effects of substrate and cytokines (IL-1β + TGF-β1 + TNF-α) on (**B**) HA and (**C**) PRG4 secretion rates, *n* =4. **D**: Correlation of secretion rates of HA and PRG4.

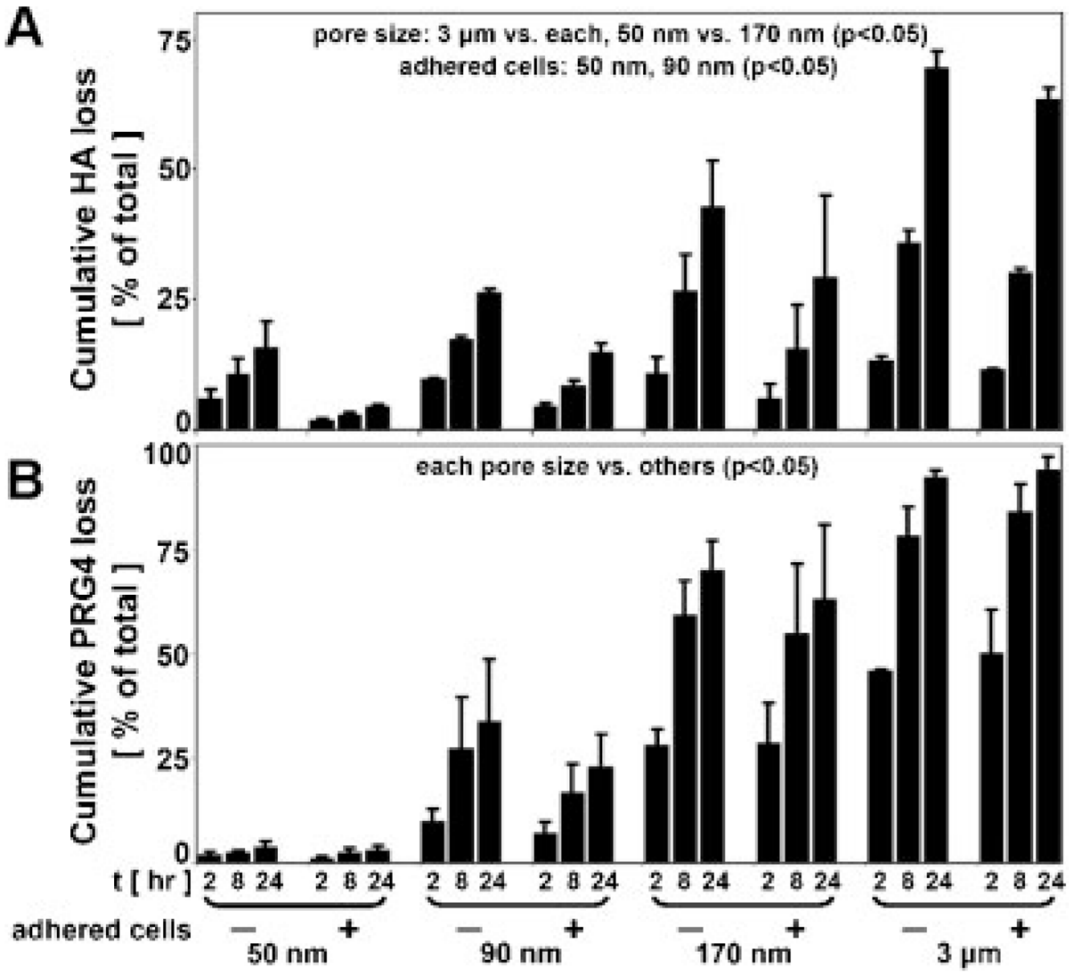

Figure 3.

(**A**) HA loss (with the mixture of MWs) and (**B**) PRG4 loss from the BF compartment into NF due to transport across indicated membranes ± adhered cells as a % of total, *n* =3–4.

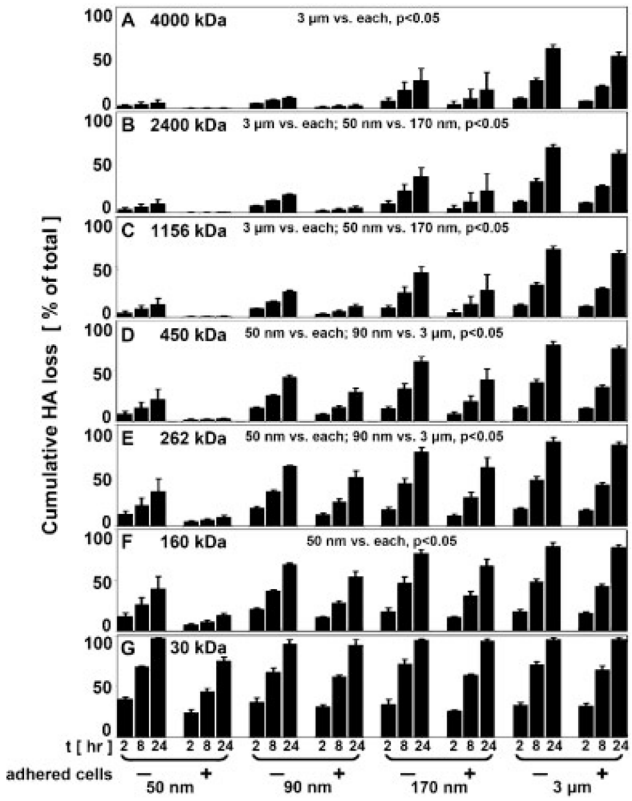

Figure 4.

HA loss, as a function of HA MW, from the BF compartment into NF due to transport across indicated membranes ± adherent cells, (**A**) 4,000, (**B**) 2,400, (**C**) 1,156, (**D**) 450, (**E**) 262, (**F**) 160, and (**G**) 30 kDa, *n* =3–4.

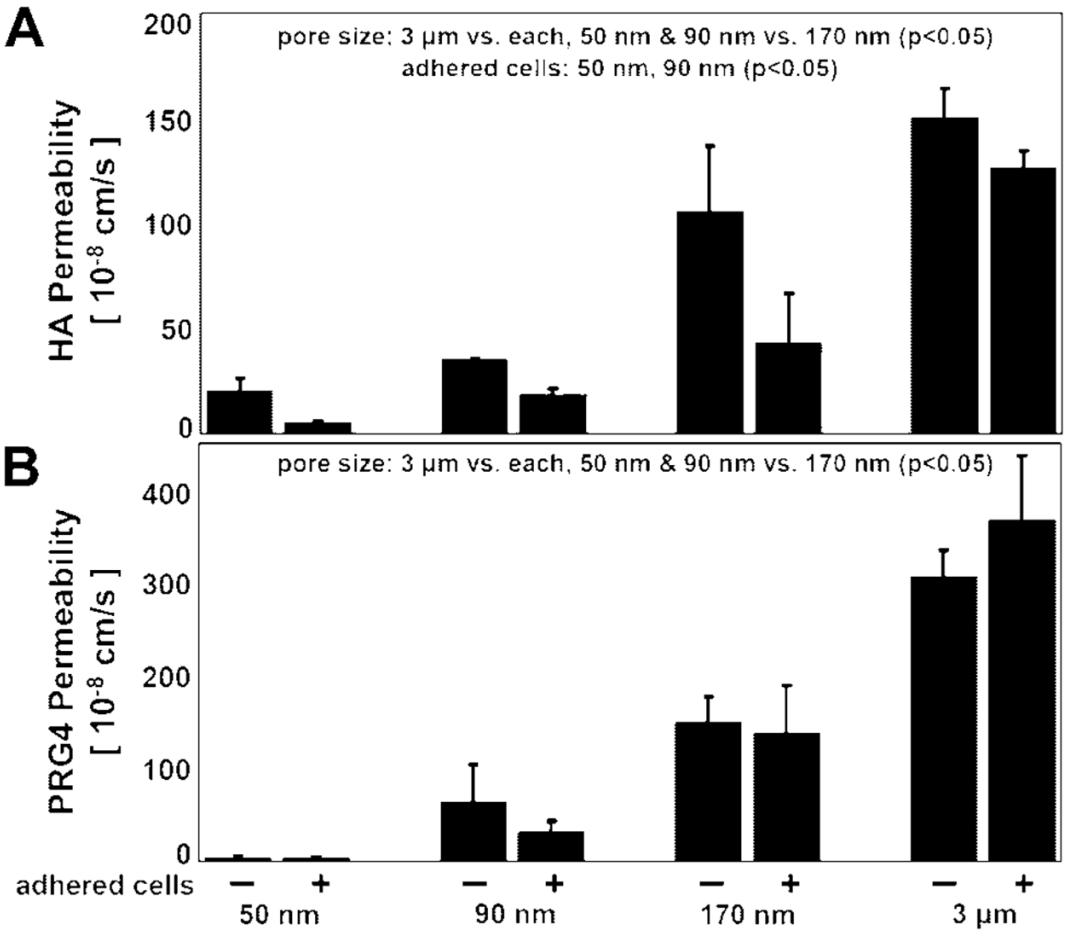

Figure 5.
Permeability of ePTFE membranes ± adhered cells to (**A**) HA (with mixture of MWs) and (**B**) PRG4, *n* =3–4.

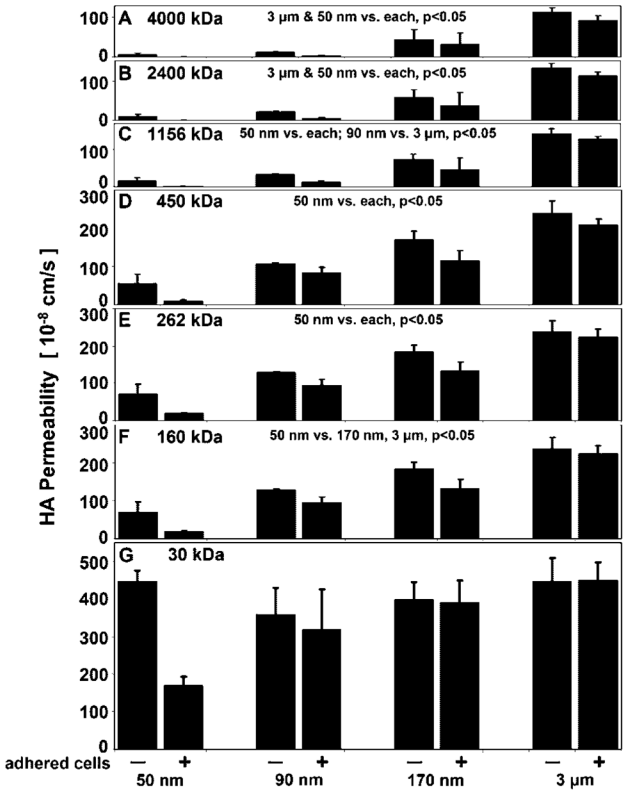

Figure 6.

Permeability of ePTFE membranes ± adherent cells to HA, as a function of HA MW, (**A**) 4,000, (**B**) 2,400, (**C**) 1,156, (**D**) 450, (**E**) 262, (**F**) 160, and (**G**) 30 kDa, *n* =3–4.

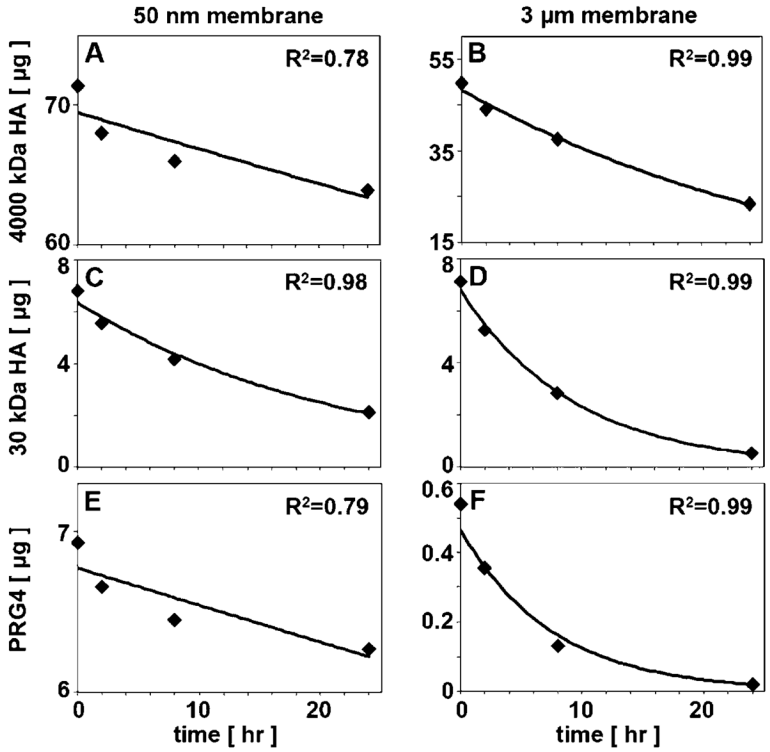

Figure 7.

Representative data of the mass of lubricant in BF vs. time (0, 2, 8, and 24 h time points) fit with exponential curves predicted by engineering analysis utilized in permeability calculations: (**A**) 4,000 kDa HA with 50 nm membranes, (**B**) 4,000 kDa HA with 3 μm membranes, (**C**) 30 kDa HA with 50 nm membranes, (**D**) 30 kDa HA with 3 μm membranes, (**E**) PRG4 with 50 nm membranes, (**F**) PRG4 3 μm membranes.

Table I

Permeability of membranes ± adherent cells to (A) HA and (B) PRG4, calculated from lubricant transport studies.

	Permeability (10^{-8} cm/s)							
	50 nm		90 nm		170 nm		3 μ;m	
	− Cells	+ Cells	− Cells	+ Cells	− Cells	+ Cells	− Cells	+ Cells
(A) HA								
MW (kDa)								
Total HA	19.6 ± 6.9	4.8 ± 0.6	34.5 ± 1.1	18.5 ± 2.5	105.5 ± 31.7	42.5 ± 24.4	150.4 ± 14.2	126.5 ± 8.3
4,000	6.4 ± 3.0	0.4 ± 0.2	11.6 ± 2.0	3.1 ± 1.4	45.0 ± 24.8	31.6 ± 29.7	113.6 ± 11.2	93.1 ± 11.1
2,400	10.6 ± 5.2	0.5 ± 0.3	21.7 ± 1.9	5.9 ± 2.2	58.1 ± 19.3	38.0 ± 32.7	132.6 ± 11.5	113.4 ± 9.1
1,156	16.1 ± 8.1	0.7 ± 0.3	33.3 ± 1.7	12.7 ± 3.0	73.5 ± 14.6	45.4 ± 31.7	142.3 ± 13.6	127.6 ± 8.3
450	31.3 ± 15.4	2.3 ± 0.5	68.3 ± 3.7	41.7 ± 7.1	114.0 ± 14.8	70.7 ± 24.7	181.8 ± 19.9	163.1 ± 12.3
262	55.1 ± 23.9	9.2 ± 2.4	106.3 ± 2.7	82.4 ± 14.8	169.8 ± 22.2	114.0 ± 27.0	238.8 ± 32.5	208.7 ± 15.3
160	71.2 ± 26.1	18.8 ± 2.5	128.4 ± 2.9	94.6 ± 15.1	184.3 ± 17.4	131.7 ± 24.3	237.2 ± 30.5	224.1 ± 20.4
30	447.6 ± 28.8	170.2 ± 22.3	358.9 ± 70.7	317.5 ± 109.2	399.4 ± 46.9	389.8 ± 59.1	447.4 ± 62.7	449.6 ± 48.2
(B) PRG4	3.9 ± 1.8	3.3 ± 1.4	63.8 ± 39.5	31.7 ± 12.4	149.4 ± 28.1	137.8 ± 51.8	305.1 ± 29.8	366.4 ± 68.9